EB2020-EBS-010

BRAKE PARTICLE MOVEMENT INSIDE THE FRICTIONAL SYSTEM

Katharina Kolbeck*[1,2], Prof. Klaus Augsburg[2]

[1]*BMW Group,*
Knorrstraße 147, 80788 München, Germany (E-mail: katharina.kolbeck@bmw.de)

[2]*Technical University of Ilmenau, Department of Automotive Engineering*
Ehrenbergstraße 15, 98693 Ilmenau, Germany

https://doi.org/10.4672/EB2020-EBS-010

ABSTRACT: Particulate pollution caused by traffic is an important socio-political issue nowadays. In addition to the engines as a source of particulate matter, non-exhaust sources of vehicles like tire, road abrasion and the brake are moving into focus due to the improved exhaust after-treatment and electrification. Although many studies have looked into brake particle number, mass and size distribution until now, the formation of this particles and their change within the frictional contact haven't been completely revealed. However, the understanding of these mechanisms is important. This knowledge can help, for example, to identify possible reduction potentials. In order to achieve a better understanding about the mechanisms that occur between the brake pad and the brake disc, tests are carried out on a tribological brake test rig. Using a borosilicate glass disc instead of a cast iron disc, allows optical in-situ measurements with a high-speed camera equipped with a magnification lens. This microscopic system can be moved horizontally and vertically with a double linear bearing. Therefore sequential observation of the entire brake pad is feasible. In addition, 3-D images provide insights into the influence of the local structure of the pad. Besides, a newly developed sampling method will be used to remove wear mass from the system and to analyze the surface below. This procedure can also be applied in combination with a grey cast iron disc, which allows further validation of the described glass method. By recording of the pad surface section by section, insights about the distribution of the brake particle movement within the tribological system can be gained. Hereby it can be analyzed, whether only the location on the pad influences the occurrence of particle motion or also other influencing variables exist. For instance, the presence of primary and secondary patches, as well as deposited wear mass and the surface morphology are important. The 3-D images can shed light on the mechanisms of wear mass deposition. Therefore this study shows new findings about brake particle behavior with regard to pad location and surface.

KEY WORDS: brake particle, frictional contact, particle movement, optical in-situ measurements, patch recognition, neuronal network

1. Introduction

Traffic is one of the most important source of anthropological particle emission. The amount of particles from the engine has been reduced in recent years through better exhaust gas after-treatment due to stricter legislation. As a result, the share of so-called non exhaust particles is almost as large as that of exhaust particles and will exceed it in the future. Sources of these particles are tire, road abrasion and brake. The latter is considered to be very important, because brake particles are a major contributor to urban particle pollution. Besides brake wear has an inhalable fraction and some constituents can have health effects. [1] Therefore a lot of studies, like [2] or [3] look into brake particle number, mass and size distribution depending on various test parameters such as speed, brake pressure or material of the friction couple. However, these results have all been obtained using different methods. Hence, another important point of current research is to define a standardized measurement setup [4–6] and a corresponding cycle similar to the WLTC [7]. However, it will also be important in the future to reduce the quantity of emitted particles. Understanding which processes take place between the two friction partners is essential. It is already known that third friction layer forms between the two friction partners. This layer is composed of the particle streams and the patches. The latter are divided into two categories, primary and secondary patches, and form the locations of the actual power transmission. Primary patches are hard elevations in the braking pad matrix. The flowing particles are redirected or even slowed down in front of them. If they accumulate there and solidify in the process, secondary patches are generated. On the secondary patches, particles can also adhere to each other to form a loosely bonded mass. This mass is then displaced by the following mass, which can also lead to movement perpendicular or against the rotation direction. In parallel to the formation of the patches, their disintegration also occurs and it is assumed that these two processes are in balance [8]. The dynamics of these processes as a function of influencing variables such as type of braking pad, pressure and other braking parameters were investigated by S. Gramstat in [9]. However, how the particles that form secondary patches are generated and how they change over time in frictional contact is not yet fully understood. Important questions are, how do the particles move, how do they influence the friction film, the formation and disintegration of patches, for example. Therefore it is first of all important to clarify where in the friction contact patch formation occurs and how large these patches are. In addition, it

must be clarified at which spots particle movement can be observed. However, since most particles and even some patches are only visible with a microscope, only a very small section of the pad can be analyzed. In order to observe the entire friction surface, the microscope is moved during the recording of a brake application and thus records the entire friction surface section by section. The resulting video is divided into smaller video clips, which are classified with the help of different neural networks regarding the presence of patches and particle motion. The term movement covers both the movement of individual particles and fibers as well as the flow of particles.

2. Test setup

2.1. Test bench

The test bench, shown in Figure 1, consists of three units with different tasks. The first part is used to represent the mechanism of braking. An engine rotates the glass disc fixed on a driving shaft and a pressure cylinder pushes the braking pad mounted inside a brake pad adapter. The braking pad is a serial ECE copper-free pad of a 17'' brake. The glass disc is made of Borofloat glass and has a diameter of 350 mm and a thickness of 6.5mm.

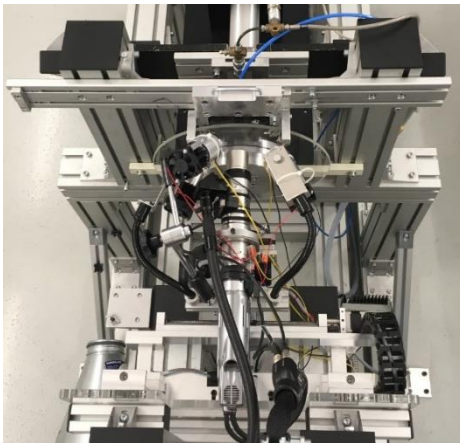

Figure 1 Overview of the test bench of TU Ilmenau

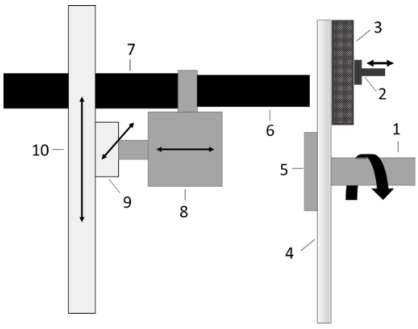

1. Drive shaft
2. Piston
3. Braking pad
4. Glass disc
5. Glass disc mounting
6. Lens
7. High-speed camera
8. Focus motor
9. Horizontal axis of traverse
10. Vertical axis of traverse

Figure 2 Sketch of the side view of the test bench including directions of movement

The Keyence microscope high-speed camera VW9000 and three high-performance LEDs are the recording unit. With this setup, recordings with 100x to 1000x magnification and a frame rate of 30 to 1000 fps are possible. The microscope also enables 3-D images, so that local structures on the surface can be analyzed with regard to their height profile. The traverse is the last part of the test bench. As shown in Figure 2 it has a horizontal (9) and a vertical (10) axis and thereby allows movements in both directions during recording. Important control variables are the number of steps and the movement speed.

2.2. Brake pad screening

The shape of the brake pad is assumed as a rectangle of 68 mm x 64 mm. The microscope on the other hand covers a 3.05 mm x 2.28 mm section at a magnification of 100x. The lowest magnification is chosen because the sensitivity of the focus to changes in height of the pad surface increases with the magnification and it cannot be changed during recording. In order to capture the total surface of the pad the camera has to be moved during recording. Thereby the friction surface is scanned s-shaped row by row. Because the microscope can only record a maximum of 600 s at a frame rate of 30 fps, screening has to be section wise. At the selected traversing speed of 300 steps/s (horizontal and vertical) one section consists of three rows. Thus the sections start alternately on the right and left side of the pad and nine sections are necessary to record the complete pad surface. After every section a short stop for saving the video is necessary. Table 1 summarizes the parameters of the traverse and the camera for the screening procedure.

Table 1 Screening parameters

Horizontal velocity	Vertical velocity	Magnification	Framerate
300 steps/s	300 steps/s	100x	30 fps

2.3. Brake cycle

Rotational speed and pressure are held constant during recording of one section. The moving direction is clockwise. Between two sections the pressure is still 5 bar to avoid changes inside the friction contact until the start of the next section. This is also ensured by the fact that the disc isn't moving between two sections. These conditions help that the disc remains undamaged for as long as possible, thus allowing the experiment to be repeated. Moreover, stationary behavior is more likely and patches are very stable. The profiles of pressure and speed over all 9 sections are shown in Figure 3.

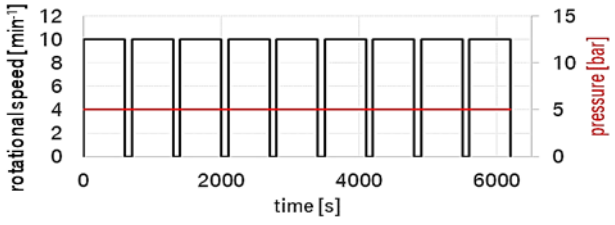

Figure 3 Speed and pressure profile over all 9 sections

2.4. Friction film removal

The friction film is removed as follows: The braking pad is moved backwards. Then a thin metal sheet equipped with an adhesive strip is inserted into the gap between the disc and the pad. When the piston is moved forward again, the pad is pressed against the adhesive strip on the sheet with the same surface pressure as before against the disc. Then the adhesive strip is first pulled off the sheet and then off the pad. Normally the patches remain on the adhesive strip so that the area under the patch on the pad surface can be analyzed. To analyses the surface before and after the removal of the friction film the 3-D function of the microscope is used. To obtain useful results, the magnification is set to 500x.

3. Video processing

3.1. Secondary Patch recognition using neural network

The detection of the patches in the screening video is done with the help of two different neuronal networks. The first one classifies the frames of the screening video into the three categories: “Patch”, “Pad Surface” and “Background”. Therefore the pretrained network ResNet18 [10] is used as the starting point and is fine-tuned to the patch classification task with hand labelled training data. Pictures that are classified as “Patch” get further processed, to determine how large the detected patch is. They are segmented with the network SegNet, which was developed at the University of Cambridge by Kendall Et al. [11]. It is a convolutional neuronal network (CNN) and consists of two different structures called encoder and decoder. To minimize the training effort the pretrained neuronal network VGG16 is used as the encoder. The entire network is then adapted to the task to distinguish between patches and background with training data for every pixel.

The original video isn't suitable input data for the neuronal networks. The video has to be split into 224 x 224 px pictures that don't overlap. Therefore a MATLAB® code cuts out six small pictures out of one frame. Four of them have the necessary size of 224 x 224 px, the other two pictures are 32 x 224 px. To get the right size the smaller pictures are extended with gray colored pixels. Both processing steps are illustrated in Figure 4.

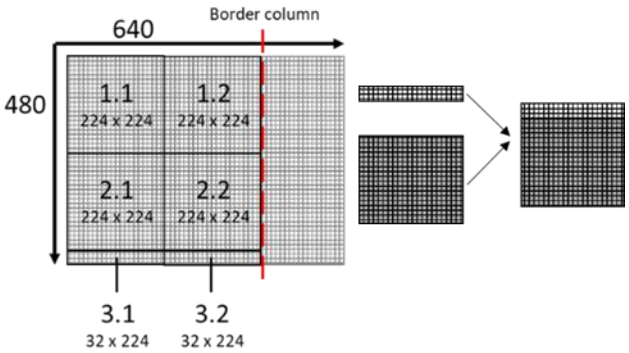

Figure 4 Splitting one frame (left) and extension of the small pictures (right)

The program then selects the next frame to be processed in the described way. This frame starts at the border column marked with a red line in Figure 4. In total 67 x 3 images with the desired size are captured per row by this procedure. Some examples of the images obtained by this way can be seen in Figure 5.

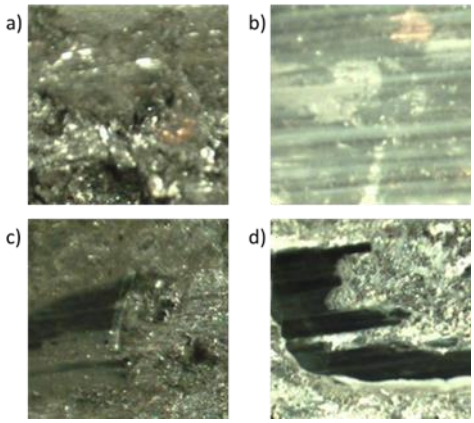

Figure 5 Examples of the small pictures for patch detection: a) Pad surface, b) scratched glass disc, c) patch, d) patch and wear mass

3.2. Motion detection using neural network

For motion detection, the video must first be converted into shorter video clips that always show the same location on the braking pad. This is only possible because the video clip frames (minor frames) are smaller parts of the original frames (major frames). These minor frames are 224 x 224 px and their position has to change with each major frame to observe the same spot on the braking pad. The shift of the minor frame per major frame has to be done contrary to the camera movement. In this way, video clips with 158 minor frames are possible. However, only clips with 150 frames are created, as this value can be converted to five whole seconds.

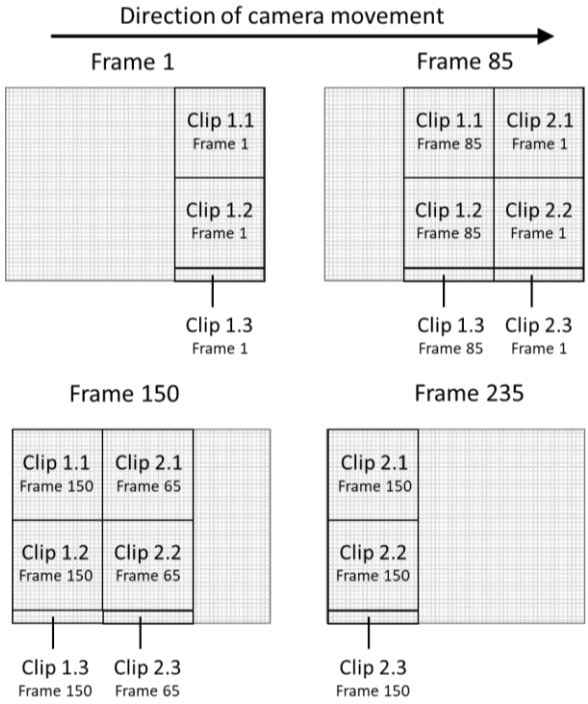

Figure 6 Position of video clips during different frames

In order to obtain clips of the edges of the braking pad, the traversing unit stops there for 5 seconds after moving down or

horizontally. Figure 6 illustrates how the positions of the first six video clips (two horizontal, three vertical), which are not at the edge of the braking pad, move during 235 frames. The minor frames of clip 3.1 and clip 3.2 that are too small, are extended with grey pixels as described in section 3.1. In total this adds up to 5427 short video clips, which show the mentioned 224 x 224 px part of the pad.

Standard convolutional neural networks are feedforward networks and don't have feedback connections. Thereby they can analyze single data points but no sequences. However, since motion can only be detected in an image sequence, a network with a feedback connection is necessary. The recurrent neural network "Long short-term memory", whose concept was first presented in 1997 by Hochreiter and Schmidbauer, has this connection [12]. To divide the video clips into the three classes background (a), no particle motion (b) and particle motion (c), a convolutional network is combined with a LSTM network. Before the network can analyze the video clip, it has to be trained with hand labelled data. To minimize the training effort the pretrained neural network "googlenet" is used as the convolutional network.

Overfitting can be avoided mainly by having a greater number of training points compared to the number of parameters of the network. In the present case the net has more than 4.8 $*10^7$ parameters and a comparable number of training points is not feasible with a reasonable amount of time. Instead the "early stopping" method is used to improve the generalization of the network.

Afterwards, all video clips of the 9 sections are classified with the trained LSTM network. For a better representation the results from the classification are converted into an image representing the scanned brake pad surface. Thereby each of the 5427 parts on the pad is colored either white (background), grey (no movement) or black (movement) according to its assigned class.

4. Results

4.1. Validation of the fine-tuned ResNet18 network

With both training and test data, the network adapted to the classification task achieves 100% accuracy in all three classes. This can be seen from the Confusion Matrices determined for both data sets in Figure 7 and Figure 8. It is highly unlikely that the network is that precise. A possible explanation would be if images from the test data were also used for the training, which can be ruled out. One other possible explanation is that the test data is very similar to the training data. Also the accumulation of surface images in both datasets could be a reason for the unexpected high accuracy.

An extension of the data with more images of the categories "Patch" and "Background" would be favorable, but the number of these images is very small. Therefore the network can only be trained after future experiments with an extended data set. For the patch detection in this work the existing trained network will be used.

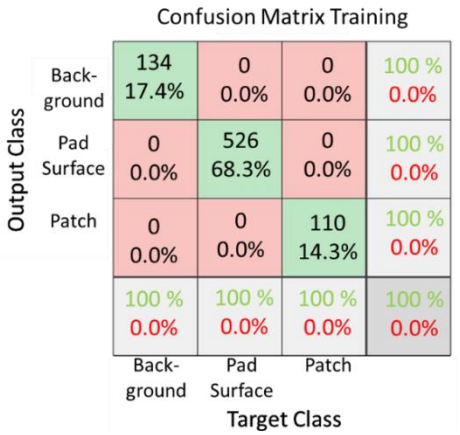

Figure 7 Training data confusion matrix of the fine-tuned ResNet Network

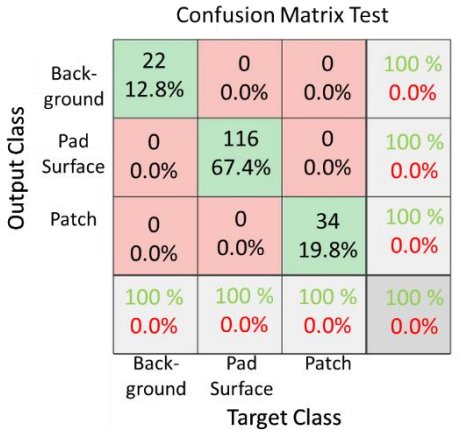

Figure 8 Test data confusion matrix of the fine-tuned ResNet Network

4.2. Validation of the SegNet Network

Figure 9 summarizes the accuracy of the trained SegNet both for the training and the test data as normalized confusion matrices. Accuracy of the test data is worse than compared to the accuracy of the training data. Overall, however, the accuracies achieved are acceptable.

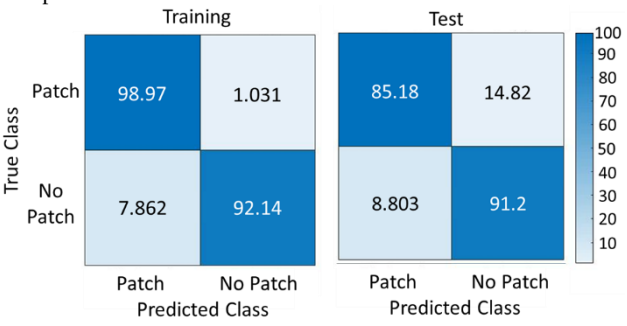

Figure 9 Normalized confusion matrices of the trained SegNet network for training and test data

4.3. Secondary Patch detection with ResNet Network

The results of the patch detection, shown in Figure 10, confirm the conclusion, that the network isn't as accurate as the confusion matrices indicate: the network detects patches at the edge of the braking pad, but they never appeared there. The verification of the

overall results with the original video shows, however, an acceptable consistence. In all three tests it can be determined that there are no patches in the upper area of the braking pad. Also in the leading side and especially in the trailing side there are hardly any patches. Instead, they accumulate strongly in the central area of the braking pad. From the results of test V3 it can also be seen that faulty detection occurs mainly when the disc is badly scratched and the small pictures then look as shown in Figure 5 b). Based on this finding, the patches determined in test V2 should also be checked again, since the disc was also significantly scratched in this test compared to test V1.

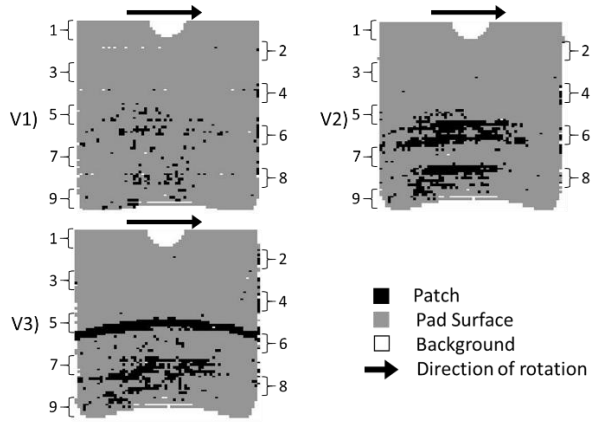

Figure 10 Results of the Patch detection of experiment 1-3 with the trained ResNet network

The comparison of the amount of images with detected patches with images without patches shows that the latter is significantly larger. In the first test 1.2 % of the images have a patch, in the second 6.7 % and in the third 7.6%.

4.4. Result of the segmentation with SegNet

In order to obtain an actual comparison between the total patch area on the braking pad and the total area of the pad surface, the images that show a patch according to the ResNet network must be segmented with the SegNet network. Two examples of such segmentation are shown in Figure 11.

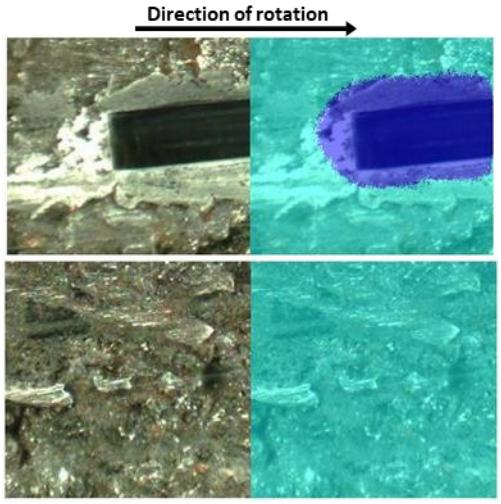

Figure 11 Examples of the segmentation with SegNet

This shows that there is still potential for optimization in terms of accuracy, as already identified in Section 4.2. However, further training data is required. The examples show that especially more images with patches are needed.

4.5. Validation of the trained LSTM Network

In order to evaluate the classification quality of the LSTM network the confusion matrix of the training data and the confusion matrix of the test data are determined. The results are summarized in Figure 12 and 13. The training data have an overall accuracy of 82.6 % and the test data have an accuracy of 78.4 %. These values are basically acceptable, but could probably be slightly improved with more training data. However, before selecting the additional training data, it should first be analyzed which video clips are often misclassified. Therefore the two Confusion Matrices are considered again. They both show that there are very few errors in the classification of the background. This was to be expected, since the background frames are significantly different from the frames showing the surface of the braking pad without motion. In this category, confusion is likely to arise if both background and pad surface (without motion) are visible in the video clip. Such clips should never have the label background. Therefore the training data should be extended with video clips with these characteristics.

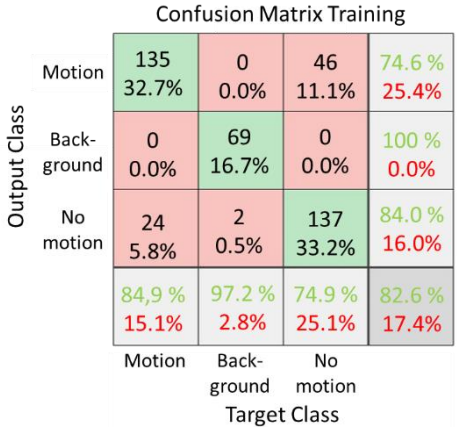

Figure 12 Training data confusion matrix of LSTM network

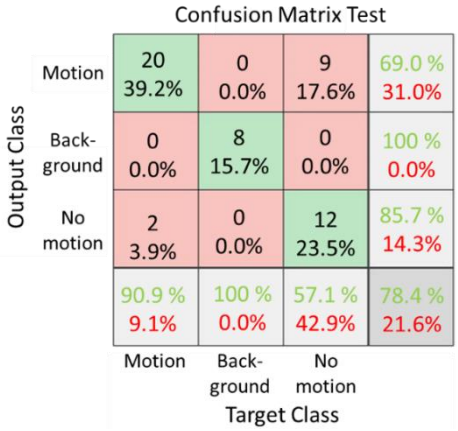

Figure 13 Test data confusion matrix LSTM network

The classification of the other two categories is significantly worse, especially for test data. The most common misclassification is for

video clips where no motion is seen, but the net seems to detect motion. Videos in which there is actually movement are much less frequently misclassified. As a result, the training data should be extended in the future, especially with video clips where no movement is visible.

Additionally, it is checked whether the extension with grey pixels has an influence on the quality of the classification. It was found that these video clips are classified incorrectly much more often. Therefore the screening strategy for future tests will be changed. Instead of moving the entire height of the section recorded by the microscope (2,28mm), the camera will only be moved down by 2.128 mm. This corresponds exactly to the 448 px covered by the video clips of lines 1 and 2. The remaining 32 px are then captured with the clip of line 1 of the next horizontal movement.

4.6. Motion detection with LSTM Network

The results of the motion detection with the trained LSTM network of three brake pad screening experiments are shown in Figure 14. In all three figures, video clips expanded with gray pixels are classified almost exclusively as ”No motion”. Even the areas at the edge of the braking pad, which actually show the background, are classified as “No motion”. Neither of them can be true. As it was mentioned before, there are two ways to minimize these errors. The change in the screening procedure as explained in the previous chapter is to be preferred.

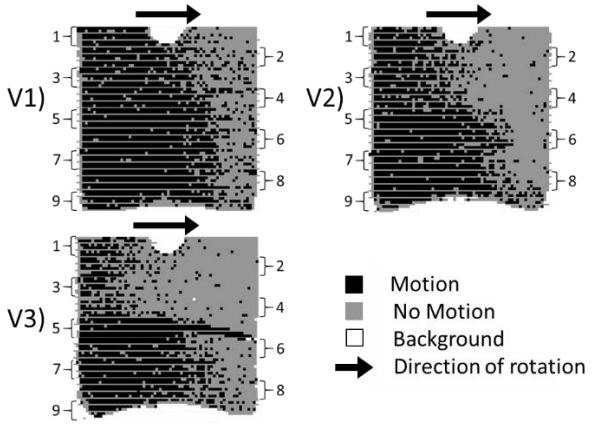

Figure 14 Results of the Motion detection of experiment 1-3 with the trained LSTM network

Overall, despite the possible classification errors, it can be stated that there is hardly any movement at the pad trailing, whereas movement is the dominant class at the leading side. However, as wear mass leaves the frictional contact, the transport of particles in the trailing part of the friction contact seems to be carried out mainly by the disc and hence, not visible on the pad surface. Furthermore, the share of areas with movement increases from the upper to the lower friction ring. This indicates that there is a dependence of the visible movement on the location on the pad surface with the present test set-up and the ECE pad used.

4.7. Motion type analysis

Beside the analysis of patch and motion distribution on the pad surface, it is important to investigate if there are different kinds of motion and under which condition motion can be detected. The unprocessed screening recordings are used for this purpose. They show that motion on the pad can be detected by the setup if one or more of the following conditions are fulfilled:

- Elevations on the pad surface in combination with a (large) particle
- Trapped wear fragments (particles and fibers)
- Partially exposed fibers of the pad matrix
- Accumulated wear mass in front of pad elevations or trapped wear fragments
- Secondary patches
- Detached wear debris on the pad surface without an elevation or a trapped wear fragment

Particles and fibers adhering to the disc can get stuck at elevations of the brake pad and thereby become visible. These areas do not have to be in contact with the disc and thus act as a primary patch. As shown in Figure 15, it is enough if the gap between the brake pad and the disc is smaller than the particle or the fiber transported by the disc. Therefore this mechanism is more likely to take place with increasing particle size and decreasing gap width.

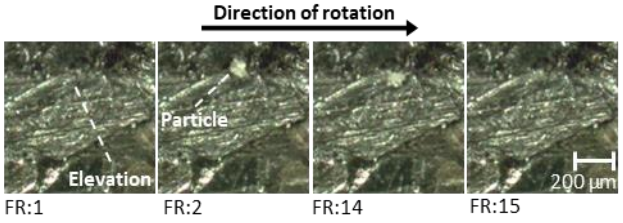

Figure 15 Particle adhering to a metallic elevation of the brake pad for 13 frames

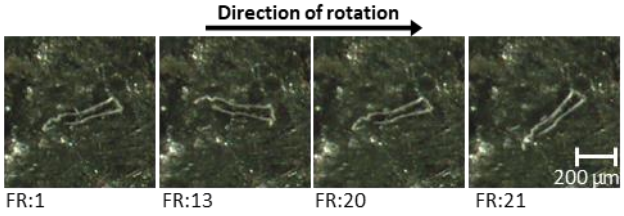

Figure 16 Movement of a trapped fiber during 21 frames

After being trapped, the particles and fibers can oscillate or rotate as illustrated in Figure 16. They can also act as a barrier to other wear fragments, which thereby become visible as well. Subsequent to this, different mechanisms can be observed. Particles can continue to move along the trapped wear fragments until there is no barrier in radial direction anymore. This mechanism is displayed in Figure 17.

Figure 17 Motion of small particles along a fiber

Furthermore, it can be observed that if a new, larger particle hits the trapped particle, its connection with the pad can loosen. The new arriving particle is thereby equal or larger compared to the trapped particle. In addition, the shear stress caused by the rotational movement of the disc can degrade the connection until it becomes loose.

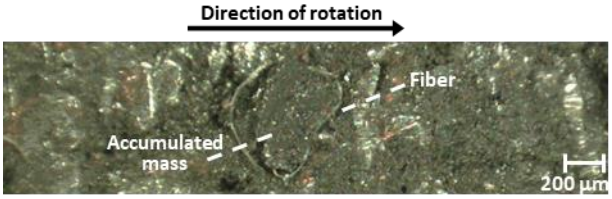

Figure 18 Accumulated wear mass formed by particles in front of a fiber

As can be seen in Figure 18, it is also possible that particles accumulate in front of trapped wear fragments as wear mass. In some cases it could even be observed that the trapped particle itself, small particles adhering to its upper surface or the wear mass accumulated in front of it can act as a secondary patch. Thus the trapped parts can have similar effects as a primary patch. An example for this is given in Figure 19. Also the formation of particles to a loosely bonded wear mass described in a previous publication [13] can occur at trapped particles. This can be seen in Figure 20. The formation of loosely bonded wear mass is more likely to occur on large particles. It would also be theoretically be possible at a fiber, but is unlikely due to its small thickness and could not be observed during the current investigations. The loosely bonded wear mass can be deposited on the surface of the pad, displace other deposits or can be removed by the disc. However, which of these processes takes place depends mainly on the structure of the surrounding pad surface.

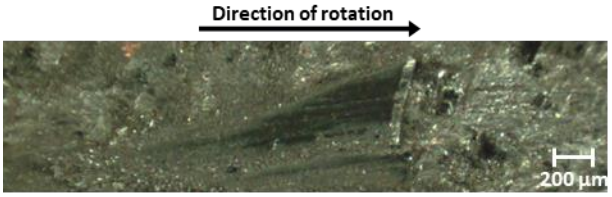

Figure 19 A secondary patch on and in front of the trapped particle

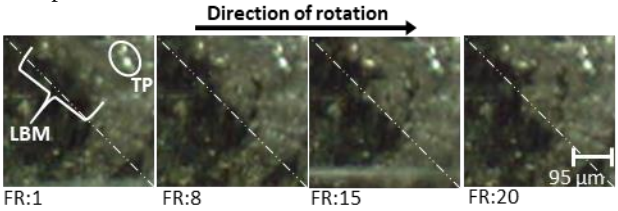

Figure 20 Moving loosely bonded wear mass (LBM) formed at a trapped particle (TP)

As mentioned above, motion can be detected at partially exposed fibers, too. Due to the fact that they show a similar behavior as the trapped fibers, the observed mechanisms are not described again.

At accumulated wear mass motion can either be observed as a particle flow around it, as Figure 21 a) shows, or in form of movement of small particles within the accumulated wear mass itself. The degree of the movement of small particles decreases with increasing solidification of the accumulated mass.

As Figure 21 b) shows, there can be a particle flow around secondary patches as well. The formation of aforementioned loosely bonded wear mass can also be observed. This mass can be pushed in different directions. After that it can be carried away by the disc, be deposited on the surface of the pad, or can further push away previously formed loosely bonded wear mass.

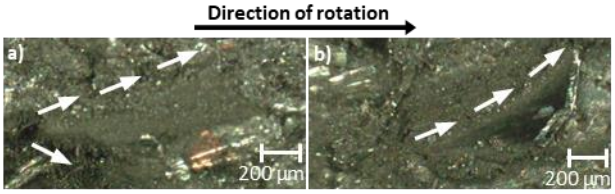

Figure 21 Particle flow around accumulated wear mass (a) and around secondary patches (b)

In some areas of the pad, depositions of wear mass occur without any trapped particle/fiber or an elevated surface area. This wear mass is labeled deposited wear debris (DWD) and where it occurs, the same motions as described previously for accumulated wear mass can be observed. This leads to the conclusion that a particle, a fiber or an elevation of the pad surface existed here before, but the compacted mass did not dissolve immediately with its removal. An example of the deposited wear debris is given in Figure 22.

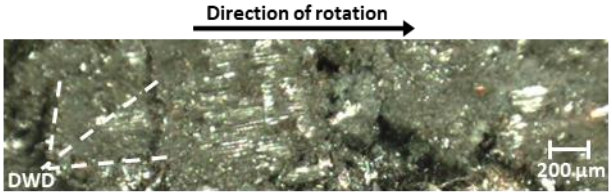

Figure 22 Deposited wear debris (DWD)

4.8. 3-D Results of friction film removal

A location on the pad surface with both a patch and bonded wear mass was selected for surface analysis after friction film removal. There was also flow movement around the patch. The condition of the surface before the removal is shown in Figure 23 both as an actual image and as a height profile. Wear mass has accumulated in front of the patch, which is the highest point (blue). The wear mass (green) is already slightly lower than the patch. The slit between the two segments of the patch, on the other hand, is almost as high as the patch areas. The places on the left side of the picture, where neither patch nor wear mass can be seen, are the lowest. After the removal, the previously viewed area is displayed in Figure 23 bottom left. Both the patch and the bonded wear mass have been detached from the pad surface by the friction film removal. Overall, the surface has changed significantly compared to the upper picture. The distinctive change in the height profile from left to right cannot be observed anymore.

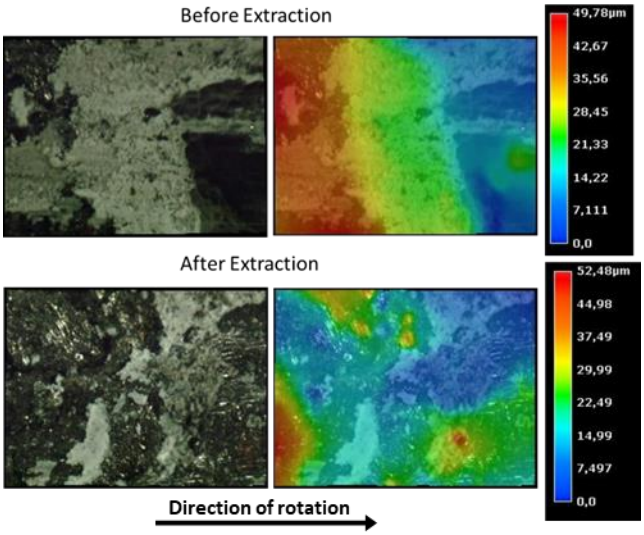

Figure 23 Results of 3-D Analysis before and after friction film removal

5. Conclusion and Outlook

The newly developed screening method in combination with different neuronal networks can provide novel information about patch and motion distribution on the braking pad surface at constant test conditions. In addition, it was possible to identify the conditions under which motion is visible on the pad surface as well as the mechanisms that occur at these spots. Therefore it is a first step towards the detection and size analysis of patches, particles and particle flows, as well as the determination of particle trajectories. In order to obtain more accurate results, the training data for the neuronal nets should be extended. In addition, the screening procedure should be improved so that the extent of misclassification decreases. For new experiments, it would also be conceivable to vary, for example, the pressure and the speed as well as the position of the piston in order to gain more information. Furthermore the procedure could be modified, so that only small sections are scanned at higher magnification. Thereby particle streams around patches and accumulated wear mass can be analyzed in detail. The LSTM network could also be extended to distinguish between the different motion categories described in section 4.5 to determine their distribution on the pad surface. The influence of the size of the trapped particles and fibers can be analyzed as well. One of the next steps should be to record videos with higher magnification at the fixed spots, where motion is detectable. Therefore the different processes like compaction, formation of loosely bonded wear mass at patches as well as the change of the particle size can be analyzed in detail. The method described here offers the possibility to locate relevant spots on the brake pad.

6. References

[1] T. Grigoratos, G. Martini. Brake wear particle emissions: a review. Environmental Science and Pollution Research, 2015, 22: 2491–2504

[2] O. Nosko, J. Vanhanen, U. Olofsson. Emission of 1.3–10 nm airborne particles from brake materials. Aerosol Science and Technology 2017, 51: 91–96

[3] J. Wahlström, L. Olander, U. Olofsson. A pin-on-disc study focusing on how different load levels affect the concentration and size distribution of airborne wear particles from the disc brake materials. Tribology letters 2012, 46: 195–204

[4] K. Augsburg, D. Hesse, F. Wenzel, G. Eichner. Measuring and characterization of brake dust particles. EuroBrake 2017 Conference Proceedings

[5] F. z. Hagen, M. Mathissen, T. Grabiec, T. Hennicke, M. Rettig, J. Grochowicz. Brake wear particle measurement setup for quantitative emission analysis. EuroBrake 2017 Conference Proceedings

[6] H. Hagino, M. Oyama, S. Sasaki. Laboratory testing of airborne brake wear particle emissions using a dynamometer system under urban city driving cycles. Atmospheric Environment 2016, 131: 269–278

[7] M. Mathissen, J. Grochowicz, C. Schmidt, R. Vogt, Farwick zum Hagen, Ferdinand H., T. Grabiec et al.. A novel real-world braking cycle for studying brake wear particle emissions. Wear 2018, 414: 219–226

[8] G.P. Ostermeyer, M. Müller. New developments of friction models in brake systems. SAE transactions 2005: 3078–3090

[9] S. Gramstat. Methoden der in-situ Visualisierung der Reibzonendynamik trockenlaufender Reibpaarungen unter Ergänzung physikalischer und chemischer Charakterisierungen der Reibpartner. Ilmenau: Universitätsverlag Ilmenau, 2015

[10] K. He, X. Zhang, S. Ren, J. Sun. Deep residual learning for image recognition. Proceedings of the IEEE Conference on Computer Vision and Pattern Recognition 2016: 770-778

[11] V. Badrinarayanan, A. Kendall, R. Cipolla. Segnet: A deep convolutional encoder-decoder architecture for image segmentation. IEEE transactions on pattern analysis and machine intelligence 2017, 39: 2481–2495

[12] S. Hochreiter, J. Schmidhuber. LSTM can solve hard long time lag problems. Advances in neural information processing 1997: 473-479

[13] K. Kolbeck, K. Augsburg. Brake particle formation and behavior in frictional contact. EuroBrake 2019 Conference Proceedings

Acknowledgement

I would like to thank Professor Klaus Augsburg for making the present investigations and my entire research project at the TU Ilmenau possible. I would also express my thanks to T. Klein for his mechanical expertise, to M. Schiele for the discussions on the subject of neural networks and to O. Frank and R. Leicht for the support.